Contents list available at IJRED website

International Journal of Renewable Energy Development

Journal homepage: https://ijred.undip.ac.id

Research Article

Performance characterization of a novel PV/T panel with nanofluids under the climatic conditions of Muscat, Oman

Afzal Husain*, Nabeel Z. Al-Rawahi, Nasser A. Al-Azri, Mohammed Al-Naabi, Musaab El-Tahir

Mechanical and Industrial Engineering Department, Sultan Qaboos University, Muscat, Oman

Abstract. The study presents an experimental analysis of a novel mini channels-based Photovoltaic/Thermal (PV/T) panel with nanofluid flow. The design consists of a PV plate attached to an aluminum substrate absorber plate having minichannels grooved on it to act as a solar collector and cooling mechanism for PV. The proposed design was tested for thermal and electrical efficiencies under the working fluids of water, Al2O3, and SiO2 nanofluids at 0.1% and 0.2% concentrations in water and at a flow rate of 0.005 l/s to 0.045 l/s. The experiments were carried out outdoors in a real environment and the measurements were taken for PV surface and fluid temperatures, incidence solar flux, electrical voltage, and current produced. The PV and PV/T performance was compared, and a noticeable enhancement in electrical efficiency was observed with the proposed design as compared to the bare PV module, and an appreciable augmentation in thermal efficiency was noticed when nanofluids were applied. The maximum electrical and thermal efficiencies of PV/T with 0.2% Al2O3 nanofluid were 19.1% and 73.4%, respectively; whereas for bare PV panels, the electrical efficiency was 18.7%. The Al2O3 nanofluid at 0.2% exhibited more than a 10% increase in thermal efficiency compared to water as a working fluid in PV/T..

Keywords: Photovoltaic/Thermal, nanofluids, aluminum absorber, minichannels, efficiency enhancement.

@ The author(s). Published by CBIORE. This is an open access article under the CC BY-SA license (http://creativecommons.org/licenses/by-sa/4.0/).

Received: 28th March 2023; Revised: 25th July 2023; Accepted: 24th August 2023; Available online: 30th August 2023

1. Introduction

Solar energy has unparalleled advantages over other renewable energy sources such as easy access, environment-friendly, abundance, and unlimited availability (Faizal *et al.*, 2013; Peng *et al.*, 2011; Zhang *et al.*, 2012; Zhao *et al.,* 2011). Oman is one of the few locations in the world where the sun is available for most of the year and with high-intensity insolation (Al-Rawahi *et al.*, 2011, 2016). The availability of solar radiation at most times of the year makes Photovoltaic (PV) systems an effective technology to harness and generate electricity in this region. PV is one of the state-of-the-art technologies that convert solar insolation directly into high-grade (electrical) energy. However, only 10% to 20% of solar energy may be used directly to generate electricity, and the remaining radiation is diffused into the surroundings (Ma *et al.,* 2015). The PV panel utilizes only the visible part of the incidence solar insolation while the infrared and other radiations go unutilized resulting in the heating up of the panel.

The efficiency, life, and durability of PV panels like any other electronics are highly dependent upon the working temperature and temperature gradients within it. A cooling mechanism can help enhance the overall performance of PV cells (Qeays *et al.,* 2020; Ragab *et al.,* 2019; Skoplaki & Palyvos, 2009; Tan & Seng, 2011). The effect of temperature on the performance of monocrystalline, polycrystalline, and amorphous PV modules is more compared to the thin film modules (Jatoi *et al.,* 2018). Ngo *et al.* (Ngo *et al.*, 2022) carried out experiments and theoretical modeling to investigate the performance of water spray-cooled PV modules in a commercial setup and observed an improvement in electrical efficiency of about 4%.

The PV/T is a hybrid system that consists of a PV module and a solar absorber. It delivers both thermal and electrical energy simultaneously (Tripanagnostopoulos et al., 2002) from solar insolation. It is an enhancement to a PV system that integrates a solar thermal collector into a PV module (Tiwari & Sodha, 2006). The thermal energy is engrossed by the flowing fluid and carried away for useful purposes (Das *et al.*, 2018; Salari *et al.*, 2021). The working fluid flows through the PV/T collector not only cools the PV panel but also carries thermal radiation leading to a temperature rise of the working fluid that can be utilized for downstream thermal processes (Adun *et al.,* 2021; Hussain *et al.*, 2019; Maadi *et al.*, 2017, 2021; Varmira *et al.*, 2021; Younis & Alhorr, 2021).

The growing energy demands and increased energy density have provided great impetus to improve the functionality and performance of the PV/T system. During the last two decades, a substantial amount of research has been carried out to design and develop an enhanced PV/T collector with higher thermal and electrical efficiencies (Al-Waeli, Sopian, *et al.*, 2017; Charalambous *et al.*, 2007; Gang *et al.*, 2011; Moradi *et al.,* 2013). The PV/T panels can be used for different applications, e.g., washing, drying, space heating, water heating, showering, and other heating applications either stand-alone or in a

* Corresponding author
Email: afzal19@squ.edu.om (A. Husain)

https://doi.org/10.14710/ijred.2023.53287
ISSN: 2252-4940/© 2023.The Author(s). Published by CBIORE

combination of other mechanical systems. The size and spacing of flow-carrying channels significantly affect the PV/T efficiency and require further investigation (Charalambous et al., 2007). The optimal flow rate of working liquid in a PV/T system can be 0.001 to 0.008 kg/s; however, it depends on the design and applications and needs further investigation (Charalambous *et al*., 2007). Further, a coverless PV/T system reduces the exergy loss and increases both electrical and thermal exergy efficiencies (Al-Shamani *et al*., 2014). The application of porous material-filled channels to cool the PV has significantly reduced the surface temperature and improved the overall system performance (Al-Masalha et al., 2023).

Both η_{elec} and η_{th} increased with the application of a roll-bond absorber plate collector in a PV module (Diwania et al., 2020). Arvind and Sodha (Tiwari & Sodha, 2006) performed experiments on a PV/T system. The authors isolated the PV module from the cooling water channel with a Tedlar film. As a result, additional thermal energy was received by the flowing water, and thermal efficiency was increased from 24% to 58%. Nijmeh *et al.* (Nijmeh *et al.,* 2022) observed a slight improvement in electrical efficiency in a PV/T compared to a PV module. The efficiency was further improved with the application of a solar concentrator to the PV/T system. Ishak et al. (Amir *et al.*, 2023) studied a bifacial PV/T with an air jet impingement cooling system. Both η_{elec} and η_{th} increased with the enhancement of flow rates. Whereas, photovoltaic exergy increased and the thermal exergy decreased with the increase in airflow rates. Further studies have shown that the airflow across the fins integrated with PV modules has increased both electrical and thermal efficiencies (Hader & Al-Kouz, 2019; Martial *et al.,* 2015).

Recently, nanofluids have been proposed as enhanced Heat Transfer Fluids (HTFs) in PV/T systems. Nanofluids absorb additional thermal energy that is falling on the PV/T module and carry it away. However, the increase in pressure loss and consequently increase in driving power with high nanofluid concentrations can be a limiting factor for its application in PV/T systems (Said *et al*., 2018). A review of the contemporary developments in PV/T systems revealed an enhancement in thermal and electrical performance compared to standalone PV systems (Garud *et al*., 2022). The most common nanofluids found in the published literature consist of Al_2O_3, CuO, ZnO, and SiO_2 particles, which have significantly enhanced both electrical and thermal efficiencies. The Al_2O_3 particle-consisting nanofluids showed a higher heat transfer coefficient followed by TiO_2, ZnO, and SiO_2 at different mass fractions (Maadi, 2017). Al-Waeli *et al.* (Al-Waeli, Chaichan, *et al.*, 2017) conducted a comparative experimental performance analysis of a PV/T in an indoor setup using water and nanofluids. The SiC-based nanofluid exhibited higher performance and efficiency compared to Al_2O_3 and CuO over a range of applied luminous intensity. The use of different nanofluids with ZnO, CuO, Al_2O_3, SiC, Hg, MgO, CeO_2, WO_2, Ti_2O_3, and ZrO_2 particles in water has observed a boost in the system efficiency by 15% to 30% (Cui *et al*., 2021).

Further numerical and experimental studies were conducted on PV/T systems using nanofluids based on Multi-Wall Carbon Nanotubes (MWCNT) (Fayaz et al., 2018). The authors observed that η_{elec} and η_{th} were enhanced by 0.064% and 5.1%, respectively, using MWCNT compared to water, and the maximum η_{th} observed was 79.1% at a nanofluid flow rate of 120 l/h. Abdallah *et al.* (Abdallah *et al.*, 2019) evaluated a water-based, low-concentration MWCNT hybrid PV/T system and observed that the performance of the PV/T systems was improved due to an increase in heat transfer coefficient, and a total efficiency of 83.62% was achieved at noon with a mean efficiency of 61.23% on a test day. The surfactants contribute significantly to improving the performance of nanofluids. Lari and Sahin (Lari & Sahin, 2017) conducted experiments on nanofluid PV/T for residential applications. The applied nanofluid consists of distilled water, Silver nanoparticles, and Potassium Oleate surfactant. An 8.5% increase in PV/T electrical output was observed with water as HTF compared to bare PV module, whereas nanofluid-cooled PV/T showed an increase of 13% compared to water-cooled PV/T.

The first and second law efficiencies of PV/T systems can be augmented by 10% to 20% by using nanofluids (Cui et al., 2021). Both entropy generation and exergy loss were reduced with the nanofluid application in PV/T systems (Sardarabadi et al., 2014). The PV/T surface temperature can be reduced by 3 to 5 °C with the use of nanofluid (Bianco et al., 2018). Also, the reduction in exergy was more significant than the entropy increase due to friction enhancement with the use of nanofluid. The nanofluids work well in high-velocity laminar flows; however, the enhancement flattens with the increase in flow rates (Abbas et al., 2019).

The absorber plate design modifications were investigated with several combinations of nanofluids. Michael and Iniyan (Michael & Iniyan, 2015b) investigated a PV/T system with copper sheet lamination using CuO-water nanofluid. The authors observed an improvement in thermal efficiency which is reaching above 45%. Khanjari et al. (Khanjari et al., 2016) utilized Ag-water and Al_2O_3-water nanofluids on a PV/T module that comprised a thermal sheet, a solar panel, a glass cover, and a 5-riser tube collector. The Ag-water nanofluid performed significantly better than the Al_2O_3-water. Al-Shamani et al. (Al-Shamani et al., 2016) performed experiments on PV/Ts and observed that SiC-water nanofluid exhibited higher efficiency (>80%) compared to TiO_2, and SiO_2 nanofluids in water which in line with the findings of Al-Waeli et al (Al-Waeli, Chaichan, *et al*., 2017). The PV/T system with Al_2O_3-water nanofluid integrated with a wavy strip improved η_{elec} and η_{th} by 3.5% and 12.1%, respectively (Maadi et al., 2021). The η_{elec} of the PV/T system was 11% higher compared to the bare PV system at a flow rate of 50 l/h with 0.1 % of CNT-nanofluid concentration (Rahmanian & Hamzavi, 2020). Michael and Iniyan (Michael & Iniyan, 2015a) proposed a novel PV/T system laminating a Cu sheet on the PV cells and using a CuO-water nanofluid. The system raised the overall efficiency by 19.25% and 11.94% with and without glazing, respectively.

Based on the above literature review, nanofluids have been extensively studied for their application in PV/T systems. Moreover, various flow configurations have been proposed to boost PV/T capabilities like copper sheet and tube collector (Maadi et al., 2017), loop pipe configuration (Cui *et al*., 2021), wavy strip (Maadi et al., 2021), and parallel channels (Abbas *et al*., 2019). It is observed that the small straight channels provide higher efficiency with manufacturing flexibility compared to standard PV/T absorbers with riser tubes. However; it has not been extensively researched to characterize and optimize its performance. Therefore, a significant gap exists in exploiting the passive enhancement techniques along with nanofluids tailored to utilize standard PV/T design and removing the efficiency enhancement bottlenecks. The current research presents new findings of a novel minichannel-based PV/T system with nanofluids.

2. Experimental Methodology and PV/T Design:

2.1 Experimental setup and data collection

The experiments were set up outdoors in the solar field at Sultan Qaboos University, Muscat, Oman, and conducted from Nov. 2021 to April 2022. The setup requires sensors, a data logger, and flow circulation for heat rejection. Fig. 1 represents

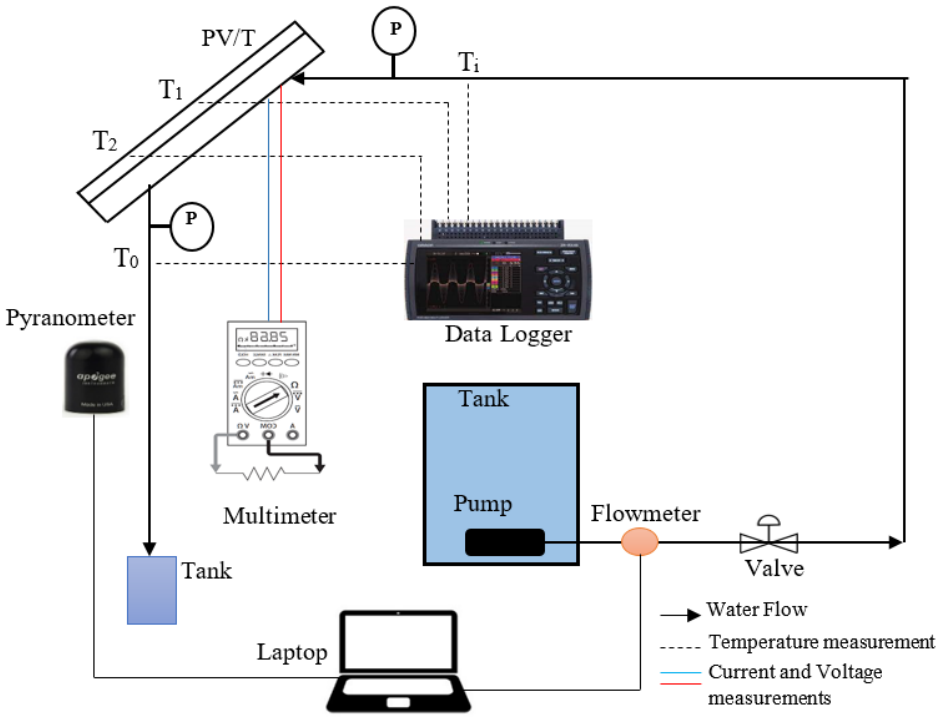

Fig. 1 Schematic of the experimental setup for the PV/T performance test

the schematic of the PV/T experimental setup. The PV panel is first fixed at an inclination of 23.35° north which is the latitude of the Muscat area for receiving maximum solar radiation (Al-Rawahi et al., 2016). The PV and PV/T panels, flow network, measurement sensors, and data logging equipment are the major elements of the experimental setup. The flow loop consists of PVC pipes, a flowmeter, a submersible pump, control valves, and a reservoir tank. The measurement and data logging consists of thermocouples, a Resistance Temperature Detector (RTD) sensor, a pyranometer, a multimeter, a data logger, and a laptop. A Hall-effect flow meter in combination with an Arduino microprocessor is used to measure the flow rate. The flow meter is accurate within ±2% error. The PicoTech PT-100 RTD sensors with PicoTech PT-104 precision data logger having an accuracy of ±0.01°C are used to monitor the fluid inlet and outlet temperatures (PicoTech, 2021). The K-type thermocouples with a data logger having an accuracy of ±1°C are used to measure the PV surface temperature. A silicon-cell-based pyranometer, manufactured by Apogee USA, which has a rapid response time of under 1 millisecond, is used to measure solar insolation. The accuracy of the pyranometer measurements is within ±4 W/m^2.

PV/T panel is connected to the flow system with the help of heavy-duty PVC pipes. The submersible pump inside the reservoir drives the flow through the flow meter, control valve, and to the PV/T panel, and the fluid after the PV/T panel is collected in a separate tank. The reservoir tank was refilled after completing a set of experiments. The calibration of the Hall-effect flow meter was done using a measurement flask and stopwatch, and the K-type thermocouples were calibrated with the RTD sensors. The experimental setup was tested and run for several hours before the first data were recorded.

2.2 PV and PV/T design

100 W monocrystalline PV panels obtained from Shanghai RAGGIE Power Co., Ltd. China (Raggie, 2021) were used in experiments. The length and width of the panel are 1200 mm and 540 mm, respectively. The rated efficiency of the solar cell is 18.3% with a maximum power tolerance of ±3%. The PV panel was dismantled and refabricated with the absorber plate having flow channels, insulation, and a frame. The absorber plate is made of a 5 mm thick A3003 aluminum substrate. The length and width of the absorber plate are kept the same as the

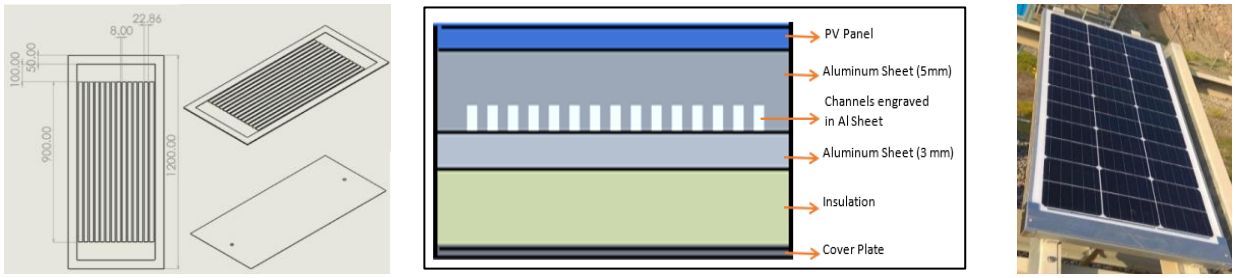

(a) (b) (c)

Fig. 2 (a) Details of the absorber plate, (b) cross-sectional details of the PV/T, and (c) assembled PV/T.

Table 1
Chemical properties of concentrated Al_2O_3-water and SiO_2-water nanofluids (US research Nanomaterials Inc.)

Characteristics	Al_2O_3	SiO_2
Appearance	White Liquid	Transparent
Crystal Structure and Type	Alpha	Amorphous
pH value	6-8	8-11
Original particle size	30nm	30nm
Nanoparticle percentage	20%	25%
Solvent	80% Water	75% water

panel. The minichannels were grooved in the aluminum substrate using a Computer Numerical Control (CNC) machine. A total of 15 channels were cut in a width of 540 mm with a gap of 22.86 mm. The width and depth of the minichannels are 8 mm and 3.4 mm, respectively as shown in Fig. 2(a). The channels were then covered with an aluminum plate followed by insulation and a wooden back cover. The thickness of the aluminum cover plate is 3 mm. The reservoirs at the ends and minichannels are set as a pathway for collector fluid to pass through the panel length. Fig. 2 shows the details of the minichannels consisting of an absorber plate, aluminum cover plate, inlet and outlet reservoirs, insulation, wooden back cover, and the PV/T assembly. The absorber plate was placed at the back of the PV cells. Thermal paste was used to provide voidless contact between the PV and absorber plate. The absorber plate is covered with the back plate having inlet and outlet ports for the working fluid. The Rockwool and wood were used as the insulation and back cover, respectively, to provide insulation and support to the panel structure.

2.3 Nanofluid Concentrations

The filtered water, Al_2O_3-water, and SiO_2-water nanofluids were used as working fluids. The desired concentrations of Al_2O_3-water and SiO_2-water nanofluids were obtained from pre-synthesized concentrated nanofluids purchased from US Research Nanomaterials, Inc., USA by diluting them with the required amount of water for experiments. The nanofluids consist of nanoparticles of size 30 nanometers with 99.99% purity immersed in water. The nanofluid solutions were subjected to sonication before application in an ultra-bath sonicator, which is a technique used to disperse the aggregated nanoparticles. Once the sonication was completed, the nanofluids were stirred on a magnetic stirrer hot plate for an hour to ensure that all the nanoparticles were properly dissolved in the solution.

The nanofluid is assumed as a homogenous mixture and the thermophysical properties are calculated based on the mixture theory.
The mixture density of the nanofluid is:

$$\rho_f = \rho_f * (1 - \phi) + \rho_p * \phi \quad (1)$$

The specific heat of the nanofluid is calculated as:

$$c_{p,nf} = \frac{\rho_f * (1-\phi)}{\rho_{nf}} * c_{p,f} + \frac{\rho_p * \phi}{\rho_{nf}} * c_{p,p} \quad (2)$$

The viscosity of the nanofluid is calculated as (Batchelor, 1977):

$$\mu_{nf} = \mu_f * (1 + 2.5 * \phi + 6.5 * \phi^2) \quad (3)$$

Maxwell's Equation (Maxwell, 1873) is used to calculate thermal conductivity:

$$k_{nf} = \frac{k_p + 2*k_f - 2*\phi*(k_f - k_p)}{\frac{k_p}{k_f} + 2 + \phi * \frac{k_f - k_p}{k_f}} \quad (4)$$

The properties of concentrated Al_2O_3-water and SiO_2-water are presented in Table 1.

3. Output Analysis

The experiments were performed for PV and PV/T panels using water and nanofluids (Al_2O_3-water and SiO_2-water). The parameters of the PV/T performance can be calculated using standard formulations (Aberoumand et al., 2018). The incidence of solar radiation can be estimated as:

$$I_G = q_{solar} \times A_{panel} \quad (5)$$

Electrical efficiency can be defined as the ratio of the power generated to the rate of energy falling on the panel:

$$\eta_{elec} = \frac{P_{elec}}{q_{solar} \times A_{panel}} \times 100\% \quad (6)$$

whereas the electric power generated can be evaluated as:

$$P_{elec} = V_{elec} \times I_{elec} \quad (7)$$

The panel is subjected to radiation and convection losses. Although a large part of the visible light is converted directly into electrical energy, some of it is reflected in the surroundings. The infrared part of the radiation is utilized to heat the working fluid and the energy is carried away. The rate of thermal energy taken away by the working fluid can be defined as:

$$\dot{Q}_c = \rho \dot{V} \, C_p \Delta T \quad (8)$$

Thermal efficiency, which is the ratio of heat carried away by water to the energy falling on the panel can be defined as:

$$\eta_{th} = \frac{\dot{Q}_c}{q_{solar} \times A_{panel}} \times 100\% \quad (9)$$

The non-dimensional quantity, temperature factor is used to characterize the panel performance, which can be expressed as:

$$\theta = \frac{T_{in} - T_a}{q_{solar}} \quad (10)$$

and the overall efficiency of the panel, which is the sum of electrical and thermal efficiency can be calculated as:

$$\eta_{overall} = \eta_{elec} + \eta_{th} \quad (11)$$

4. Results and Discussion

4.1 Solar flux and PV performance

The experiments were performed for both PV and PV/T panels using water and nanofluids to compare the performance. The time-based characteristics were obtained by conducting the experiments between 8:00 a.m. and 4:00 p.m., and the data was collected every hour. The data was collected through a series of measurements taken within 5 minutes and the averaged values were reported at that time interval. The flow rate-based characteristics were recorded by changing the flow rates of the

Table 2
Thermophysical properties of water, nanoparticles, and nanofluids (Al_2O_3-water, and SiO_2-water) at different concentrations

	Density (Kg/m^3)	Specific Heat Capacity ($J/Kg.K$)	Thermal Conductivity ($W/m.K$)	Dynamic Viscosity($\times 10^{-4}$ Pa.s)
Pure Water	997.1	4180	0.614	8.5
Al_2O_3 Nanoparticles	3600	765	36	-
0.1% Nanofluid	1000	4168	0.618	8.56
0.2% Nanofluid	1003	4156	0.622	8.58
SiO_2 Nanoparticles	6500	533	33	-
0.1% Nanofluid	1003	4156	0.618	8.56
0.2% Nanofluid	1009	4133	0.622	8.58

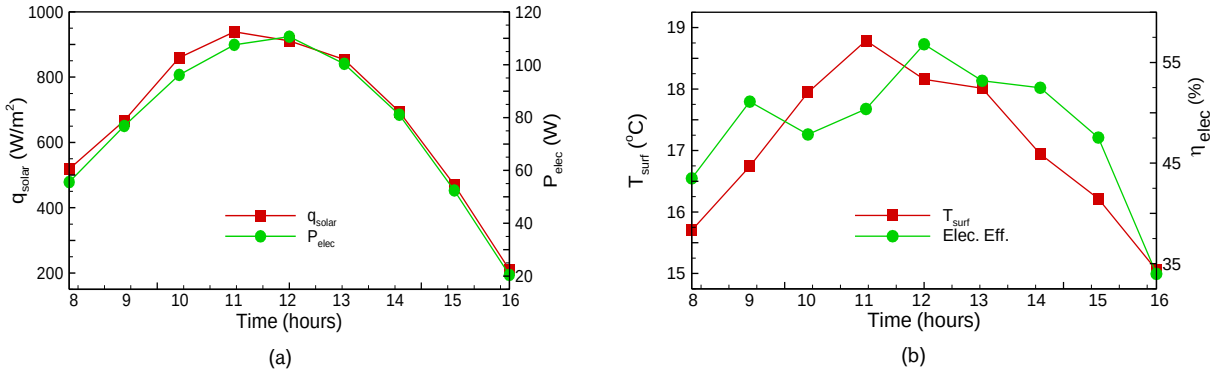

Fig. 3 Variation of (a) solar flux and power, and (b) temperature and electrical efficiency of a PV panel without cooling

working fluid during the mid-day when the solar angle is within 30 degrees from the zenith. The thermophysical properties of different concentrations of nanofluid used in experiments have been calculated using Eqs. 1 to 4 and summarized in Table 2.

The temperature and solar flux were measured and electrical efficiency and power generation were calculated using Eqs. 6 and 7. The variation of heat flux, average PV surface temperature, power generated, and electrical efficiency are presented in Fig. 3. The solar flux increases with time until the solar noon and decreases after that until sunset. The power generation follows the heat flux trend except for the peak power generation, which is delayed and occurs slightly after the solar noon. The shift of peak power generation from the peak solar flux is related to the peak electrical efficiency which is also shifted slightly away from the maximum surface temperature. The surface temperature varies as per the variation of solar flux, and the maximum temperature of 62.5 °C was recorded for a PV system without a cooling arrangement corresponding to a maximum solar flux of 938.8 W/m^2. The maximum electrical efficiency of 18.73% is obtained at the higher solar flux; however, it corresponds to the point of higher power generation. It can be observed that the power generation and efficiency reached maximum where the solar flux value is higher; however, the surface temperature is not maximum, which is in line with the efficiency and temperature relationship and exhibits that the temperature adversely affects the efficiency and power generation (Tan & Seng, 2011).

4.2 PV and PV/T performance comparison and model equations

Further experiments are performed on PV and PV/T to investigate cooling effects on electrical efficiency, solar collection, and thermal efficiency. The electrical and thermal efficiencies curves are obtained for the reduced temperature difference $(T_{in} - T_a)/q_{solar}$) using Eqs. 6 to 10 as shown in Fig. 4. The electrical efficiency decreases with the increase in temperature difference which is characteristically in line with the open literature (Skoplaki & Palyvos, 2009). The variation shows a linear relationship for both water and nanofluid as coolants (Fig. 4(a)). Similar curves were obtained for thermal efficiency against the reduced temperature difference (Figs. 4(a) and (b)). The larger value of reduced temperature causes larger global temperature differences for radiation and convection losses which results in reduced electrical and thermal efficiencies. The curves show linear relationships for both

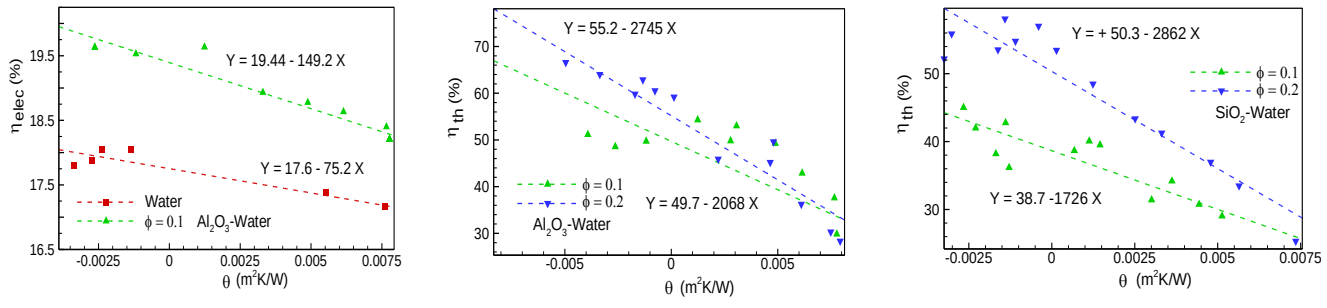

Fig. 4 Variation of PV efficiency with the change if temperature difference: (a) electrical efficiency with water and Al_2O_3-water (b) thermal efficiency with Al2O3-water, and (c) thermal efficiency with SiO2-water

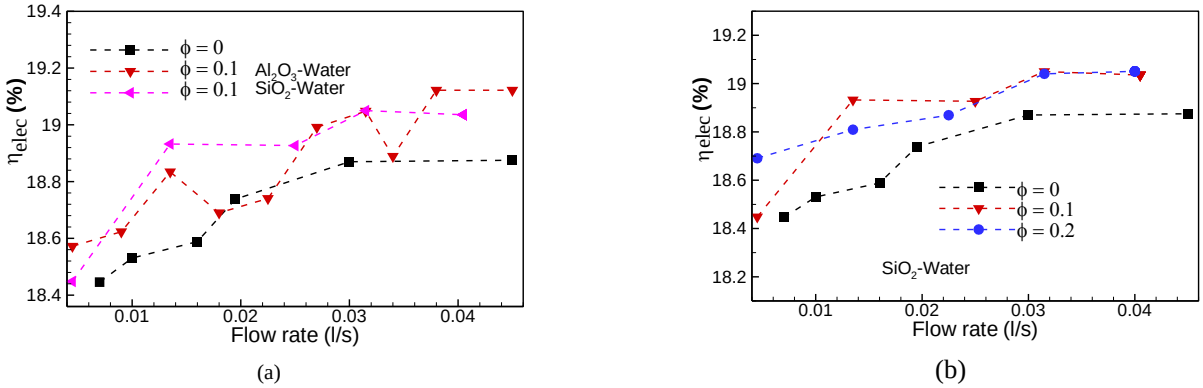

Fig. 5 Variation of PV/T electrical efficiency with the change of flow rate and coolant: (a) water, Al_2O_3-water, and SiO_2-water, (b) water and SiO_2-water

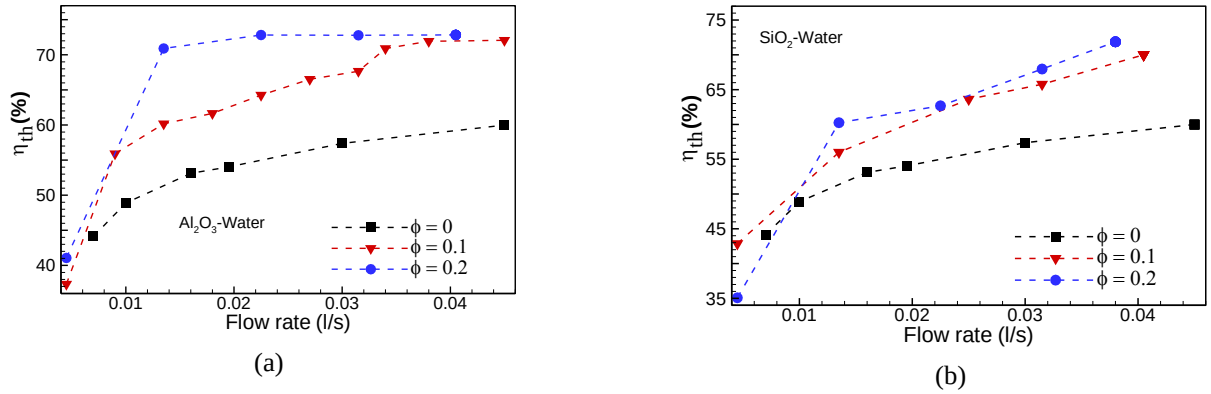

Fig. 6 Comparison of thermal efficiency with the change in flow rate of working fluids, (a) water and Al_2O_3-water, and (b) water and SiO_2-water

nanofluids, i.e., Al_2O_3-water and SiO_2-water. Several model equations are obtained based on the linear curve fitting for electrical and thermal efficiencies based on the experimental data.

For water as a working fluid, the electrical efficiency can be expressed as:

$$\eta_{elec,w} = 17.6 - 75.2\theta \quad (12)$$

For Al_2O_3-water as a working fluid, the electrical and thermal efficiencies can be presented as:

$$\eta_{elec,nf} = 19.2 - 112.7\theta \quad \phi = 0.1 \quad (13)$$
$$\eta_{th,nf} = 49.7 - 2068\theta \quad \phi = 0.1 \quad (14)$$
$$\eta_{th,nf} = 55.2 - 2745\theta \quad \phi = 0.2 \quad (15)$$

For SiO_2-water nanofluid, the thermal efficiencies can be expressed as:

$$\eta_{th,nf} = 38.7 - 1726\theta \quad \phi = 0.1, \quad (16)$$
$$\eta_{th,nf} = 50.3 - 2862\theta \quad \phi = 0.2, \quad (17)$$

4.3 Effect of flowrate and nanofluid concentrations on electrical and thermal efficiencies

The performance of the PV/T panel was investigated for the change in working fluid flow rate as shown in Figs. 5 and 6. The flow rate was varied from 0.007 l/s to 0.045 l/s to achieve a measurable temperature difference. The efficiency trends show that the electrical efficiency increases with the increase in the coolant flow rate for both water and nanofluids as shown in Fig. 5. However, the nanofluid shows more improvement in efficiency, which further increases with the increase in nanofluid concentrations. The nanofluid concentrations of 0.1 and 0.2 increase electrical efficiency by an average of 0.1 and 0.2 percent, respectively, compared to water as a working fluid. The maximum η_{elec} of 19.1% is obtained for PV/T under a solar flux of 1016 W/m^2 with Al_2O_3-water nanofluid with $\phi = 0.2$.

Similar trends are obtained for the thermal efficiency of PV/T with the change in flow rates as shown in Fig. 6. The η_{th} increases sharply in the beginning; however, the curve flattens with a further increase in flow rates for all working fluids investigated in this study. The nanofluids show significantly higher η_{th} compared to water and it increases further with the increase in nanofluid concentrations. The Al_2O_3-water nanofluid shows higher thermal efficiency compared to SiO_2-water as a working fluid. The thermal efficiency enhancement was more than 10% at higher flow rates. The maximum η_{th} of 73.4% is obtained for PV/T under a solar flux of 1016 W/m^2 with Al_2O_3-water nanofluid. The thermal efficiency gap between water and nanofluids increases with the increase in nanofluids concentrations. However, the higher efficiencies using the nanofluid come along with the higher pressure drops (Adun et al., 2021), and trade must be investigated to take advantage of the nanofluid application.

The $\eta_{overall}$ that represents the summation of η_{elec} and η_{th} increases with an increase in flow rates (Fig. 7). Similar to the trends of η_{elec} and η_{th}, the $\eta_{overall}$ increases sharply at the beginning and the curve flattens with further increases in flow rates. The nanofluids show higher efficiency compared to water and it increases further with the increase in nanofluid concentrations. The characteristics of the overall thermal efficiency are dominated by the η_{th} as the magnitude of thermal efficiency is much higher compared to electrical efficiency. The Al_2O_3-water shows greater overall efficiency compared to SiO_2-water. The

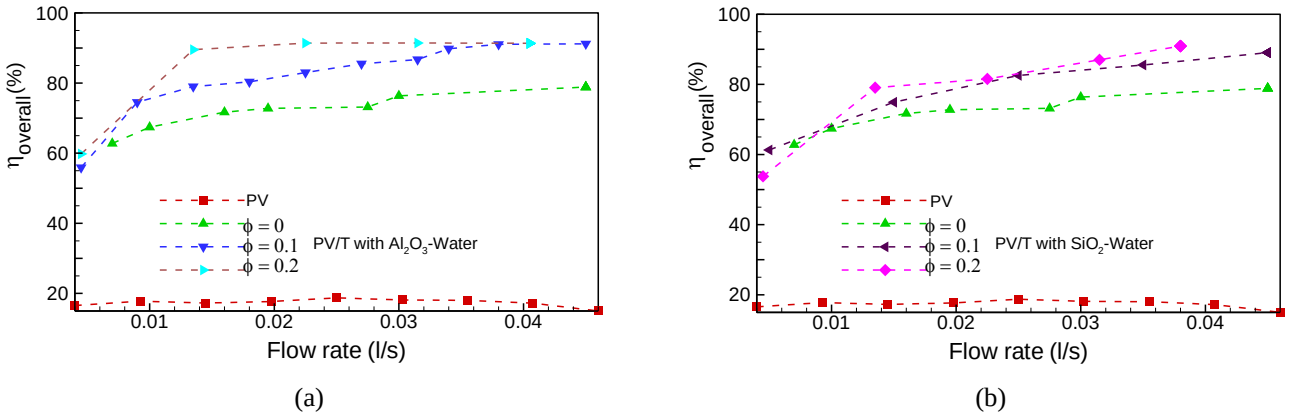

Fig. 7 Comparison of overall efficiency with the change in flow rate of working fluids, (a) Water and Al_2O_3-water, and (b) water and SiO_2-water

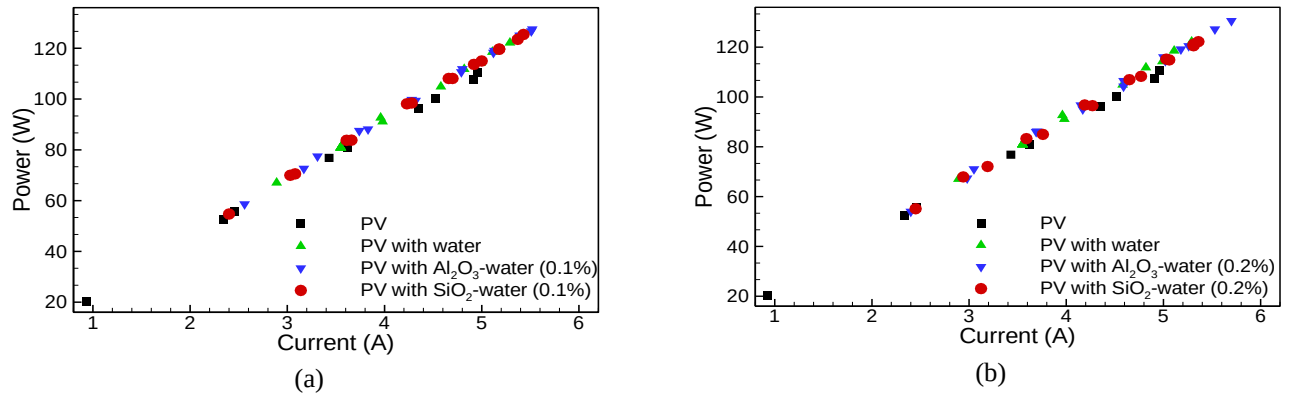

Fig. 8 P-I characteristics of PV and PV/T panels with water, Al_2O_3-water and SiO_2-water at (a) ϕ = 0.1% and (b) ϕ = 0.2%

maximum $\eta_{overall}$ of 91.2% is obtained for PV/T under a solar flux of 1016 W/m^2 with Al_2O_3-water nanofluid.

3.4 Power-current (P-I) characteristics

The P-I characteristics of PV and PV/T panels are shown in Fig. 8. Water, Al_2O_3-Water, and SiO_2-Water nanofluids are used as working fluids with 0.1% and 0.2% concentrations. The results presented the variation of current and corresponding power with the change of solar flux. The generated current increases which consequently increases the generated power monoto nously with the increase in the incidence of solar flux.

4. Conclusions

The study proposes a novel absorber plate integrated with a PV panel to provide PV cooling as well as solar thermal energy collection. The proposed absorber plate is made of aluminum substrate grooved with minichannels, inlet and outlet reservoirs, and a cover plate. The PV cells with tedlar film are attached to the absorber plate and assembly is completed providing back insulation. The experiments were conducted outdoors to measure the electrical power produced and thermal energy collection, and to characterize the performance of the proposed PV/T panel with water and nanofluids. The PV and PV/T are tested for daytime performance as well as performance with the change of working fluids flow rates.

The electrical efficiency of the PV follows the pattern of an increase and decrease with solar flux during a sunny day. At a certain point, the electrical efficiency decreases with the increase in PV temperature due to an increase in solar flux, which results in a decrease in electrical efficiency even at high solar flux. The PV electrical efficiency varied from 14.99% to 18.75% during a day operation. Both electrical and thermal efficiencies reduce with the increase in inlet temperature of the working fluid, and both water and nanofluid show similar trends. The higher flow rate of the working fluid reduces the temperature rise of the PV and consequently reduces the thermal losses, which increases both electrical and thermal efficiencies. The PV/T system reduces the maximum surface temperature by 14 °C compared to the PV module. The thermal efficiency further increases with the increase in nanofluid particle concentrations. The increase in solar flux increases PV current generation and consequently power generation linearly in the range investigated in this study. The average electrical efficiency of the PV/T system with 0.2% Al_2O_3-water was 3.75% higher compared to the PV module during its operation from 9:00 a.m. to 3:00 p.m.

The power produced in the PV module is linearly related to the current generated in the cell, which is changed monotonously with solar flux. The thermal efficiency shows significant improvement with nanofluid over water, however, the change in electrical efficiency was insignificant with the change of working fluid from water to nanofluids. The nanofluid, though, increases the thermal efficiency significantly, it causes an additional pressure drop in the system and requires utmost care and trade-off in the nanofluid application, which needs further investigation for nanofluid pressure drop, exergy loss, and power consumption.

Nomenclature

I_G	Incidence solar radiation
Q_{solar}	Solar flux
A_{panel}	Panel surface area subjected to solar radiation

P_{elec}	Electrical power
V_{elec}	Electrical voltage
I_{elec}	Electrical current
$\dot{Q}_c$	Rate of heat energy carried away by water
ρ	Density of working fluid
$\dot{V}$	Volume flow rate of working fluid
C_p	Specific heat of the working fluid
T	Temperature
ΔT	Temperature difference
η_{elec}	Electrical efficiency
η_{th}	Thermal efficiency
$\eta_{overall}$	Overall efficiency
$\eta_{elec,w}$	Electrical efficiency of PV/T with water as the working fluid
$\eta_{elec,nf}$	Electrical efficiency of PV/T with nanofluid as the working fluid
$\eta_{th,nf}$	Thermal efficiency of PV/T with nanofluid as working fluid
θ	Temperature factor
ϕ	Nanofluid mass fraction

Acknowledgments

The authors acknowledge the support from Sultan Qaboos University, Oman, (Grant No. (IG/ENG/MEID/21/01), and the Ministry of Higher Education, Research and Innovation (RC/URG-ENG/MIED/21/01) for funding this research.

Author Declarations

Authors have no conflict to disclose

References

Abbas, N., Bilal, M., Amer, M., Muhammad, S., Sajjad, U., Muhammad, H., Zahra, N., Hussain, M., Badshah, M. A., & Turab, A. (2019). Applications of nanofluids in photovoltaic thermal systems : A review of recent advances. *Physica A*, *536*, 122513. https://doi.org/10.1016/j.physa.2019.122513

Abdallah, S. R., Saidani-Scott, H., & Abdellatif, O. E. (2019). Performance analysis for hybrid PV/T system using low concentration MWCNT (water-based) nanofluid. *Solar Energy*, *181*(October 2018), 108–115. https://doi.org/10.1016/j.solener.2019.01.088

Aberoumand, S., Ghamari, S., & Shabani, B. (2018). Energy and exergy analysis of a photovoltaic thermal (PV / T) system using nano fl uids : An experimental study. *Solar Energy*, *165*(January), 167–177. https://doi.org/10.1016/j.solener.2018.03.028

Adun, H., Adedeji, M., Dagbasi, M., Bamisile, O., Senol, M., & Kumar, R. (2021). A numerical and exergy analysis of the effect of ternary nanofluid on performance of Photovoltaic thermal collector. *Journal of Thermal Analysis and Calorimetry*, *145*(3), 1413–1429. https://doi.org/10.1007/s10973-021-10575-y

Al-Masalha, I., Ujila, S., Masuri, B., Badran, O., Anuar, M. K., Ariffin, M., Rahim, A., Talib, A., & Alfaqs, F. (2023). *Theoretical and Experimental Study on the Performance of Photovoltaic using Porous Media Cooling under Indoor Condition*. *12*(2), 313–326. https://doi.org/10.14710/ijred.2023.47686

Al-Rawahi, N. Z., Zurigat, Y. H., & Al-azri, N. A. (2016). Investigating different diffuse solar radiation models to analyse solar radiation on inclined surfaces in Oman. *International Journal of Sustainable Energy*, *35*(8), 757–773. https://doi.org/10.1080/14786451.2014.950961

Al-Rawahi, N. Z., Zurigat, Y. H., & Al-Azri, N. A. (2011). Prediction of hourly solar radiation on horizontal and inclined surfaces for Muscat/Oman. *Journal of Engineering Research*, *8*(2), 19–31. https://doi.org/10.24200/tjer.vol8iss2pp19-31

Al-Shamani, A. N., Sopian, K., Mat, S., Abdulrasool, H., Abed, A. M., & Ruslan, M. H. (2016). Experimental studies of rectangular tube absorber photovoltaic thermal collector with various types of nanofluids under the tropical climate conditions. *Energy Conversion and Management*, *124*, 528–542. https://doi.org/10.1016/j.enconman.2016.07.052

Al-Shamani, A. N., Yazdi, M. H., Alghoul, M. A., Abed, A. M., Ruslan, M. H., Mat, S., & Sopian, K. (2014). Nanofluids for improved efficiency in cooling solar collectors – A review. *Renewable and Sustainable Energy Reviews*, *38*, 348–367. https://doi.org/10.1016/j.rser.2014.05.041

Al-Waeli, A. H. A., Chaichan, M. T., Kazem, H. A., & Sopian, K. (2017). Comparative study to use nano- (Al 2 O 3 , CuO , and SiC) with water to enhance photovoltaic thermal PV / T collectors. *Energy Conversion and Management*, *148*, 963–973. https://doi.org/10.1016/j.enconman.2017.06.072

Al-Waeli, A. H. A., Sopian, K., Kazem, H. A., & Chaichan, M. T. (2017). Photovoltaic/Thermal (PV/T) systems: Status and future prospects. *Renewable and Sustainable Energy Reviews*, *77*(November 2016), 109–130. https://doi.org/10.1016/j.rser.2017.03.126

Amir, M., Bin, A., Ibrahim, A., Sopian, K., Fauzan, M. F., Rahmat, A. A., Jannah, N., & Yusaidi, B. (2023). Performance and economic analysis of a reversed circular flow jet impingement bifacial PVT solar collector. *International Journal of Renewable Energy Development*, *12*(4), 780–788. https://doi.org/10.14710/ijred.2023.54348

Batchelor, G. K. (1977). The effect of Brownian motion on the bulk stress in a suspension of spherical particles. *Journal of Fluid Mechanics*, *83*(1), 97–117. https://doi.org/10.1017/S0022112077001062

Bianco, V., Scarpa, F., & Tagliafico, L. A. (2018). Numerical analysis of the Al2O3-water nanofluid forced laminar convection in an asymmetric heated channel for application in flat plate PV/T collector. *Renewable Energy*, *116*, 9–21. https://doi.org/10.1016/j.renene.2017.09.067

Charalambous, P. G., Maidment, G. G., Kalogirou, S. A., & Yiakoumetti, K. (2007). Photovoltaic thermal (PV / T) collectors : A review. *Applied Thermal Engineering*, *27*, 275–286. https://doi.org/10.1016/j.applthermaleng.2006.06.007

Cui, Y., Zhu, J., Zoras, S., & Zhang, J. (2021). Comprehensive review of the recent advances in PV / T system with loop-pipe configuration and nanofluid. *Renewable and Sustainable Energy Reviews*, *135*(April 2020), 110254. https://doi.org/10.1016/j.rser.2020.110254

Das, D., Kalita, P., & Roy, O. (2018). Flat plate hybrid photovoltaic-thermal (PV / T) system : A review on design and development. *Renewable and Sustainable Energy Reviews*, *84*(October 2017), 111–130. https://doi.org/10.1016/j.rser.2018.01.002

Diwania, S., Agrawal, S., Siddiqui, A. S., & Singh, S. (2020). Photovoltaic – thermal (PV / T) technology : a comprehensive review on applications and its advancement. *International Journal of Energy and Environmental Engineering*, *11*(1), 33–54. https://doi.org/10.1007/s40095-019-00327-y

Faizal, M., Saidur, R., Mekhilef, S., & Alim, M. A. (2013). Energy , economic and environmental analysis of metal oxides nanofluid for flat-plate solar collector. *Energy Conversion and Management*, *76*, 162–168. https://doi.org/10.1016/j.enconman.2013.07.038

Fayaz, H., Nasrin, R., Rahim, N. A., & Hasanuzzaman, M. (2018). Energy and exergy analysis of the PVT system: Effect of nano fluid flow rate. *Solar Energy*, *169*(May), 217–230. https://doi.org/10.1016/j.solener.2018.05.004

Gang, P., Huide, F., Tao, Z., & Jie, J. (2011). A numerical and experimental study on a heat pipe PV/T system. *Solar Energy*, *85*(5), 911–921. https://doi.org/10.1016/j.solener.2011.02.006

Garud, K. S., Hwang, S.-G., Han, J.-W., & Lee, M.-Y. (2022). Symmetry Review on Performance Enhancement of Photovoltaic / Thermal – Thermoelectric Generator Systems with Nanofluid Cooling. *Symmetry* *14*(1), 2–22. https://doi.org/10.3390/sym14010036

Hader, M., & Al-Kouz, W. (2019). Performance of a hybrid photovoltaic/thermal system utilizing water-Al2O3 nanofluid and fins. *International Journal of Energy Research*, *43*(1), 219–230. https://doi.org/10.1002/er.4253

Hussain, M. I., Kim, J. H., & Kim, J. T. (2019). Nanofluid-powered dual-fluid photovoltaic/thermal (PV/T) system: Comparative numerical study. *Energies*, *12*(5), 775. https://doi.org/10.3390/en12050775

Jatoi, A. R., Samo, S. R., & Jakhrani, A. Q. (2018). Influence of Temperature on Electrical Characteristics of Different Photovoltaic Module Technologies. *International Journal of Renewable Energy Development*, *7*(2), 85–91. https://doi.org/10.14710/ijred.7.2.85-91

Khanjari, Y., Pourfayaz, F., & Kasaeian, A. B. (2016). Numerical

investigation on using of nanofluid in a water-cooled photovoltaic thermal system. *Energy Conversion and Management*, *122*, 263–278. https://doi.org/10.1016/j.enconman.2016.05.083

Lari, M. O., & Sahin, A. Z. (2017). Design , performance and economic analysis of a nano fl uid-based photovoltaic / thermal system for residential applications. *Energy Conversion and Management*, *149*(April), 467–484. https://doi.org/10.1016/j.enconman.2017.07.045

Ma, T., Yang, H., Zhang, Y., Lu, L., & Wang, X. (2015). Using phase change materials in photovoltaic systems for thermal regulation and electrical efficiency improvement: A review and outlook. *Renewable and Sustainable Energy Reviews*, *43*, 1273–1284. https://doi.org/10.1016/j.rser.2014.12.003

Maadi, S. R. (2017). Effects of Nanofluids Thermo-Physical Properties on the Heat Transfer and 1 st law of Thermodynamic in a Serpentine PVT System. *17th Conference On Fluid Dynamics*, 27–29.

Maadi, S. R., Kolahan, A., Passandideh Fard, M., & Sardarabadi, M. (2017). Effects of Nanofluids Thermo-Physical Properties on the Heat Transfer and 1st law of Thermodynamic in a Serpentine PVT System. *17th Conference On Fluid Dynamics, Shahrood University of Technology, Shahrood, Iran*, 27–29.

Maadi, S. R., Navegi, A., Solomin, E., Ahn, H. S., Wongwises, S., & Mahian, O. (2021). Performance improvement of a photovoltaic-thermal system using a wavy-strip insert with and without nanofluid. *Energy*, *234*(December 2015), 121190. https://doi.org/10.1016/j.energy.2021.121190

Martial, E. A. A., Njomo, D., & Agrawal, B. (2015). Thermal energy optimization of building integrated semi-transparent photovoltaic thermal systems. *International Journal of Renewable Energy Development*, *4*(2), 113–123. https://doi.org/10.14710/ijred.4.2.113-123

Maxwell, J. C. (1873). *A treatise on electricity and magnetism* (Vol. 1). Clarendon press. https://doi.org/10.1017/CBO9780511709333

Michael, J. J., & Iniyan, S. (2015a). Performance analysis of a copper sheet laminated photovoltaic thermal collector using copper oxide - water nanofluid. *Solar Energy*, *119*, 439–451. https://doi.org/10.1016/j.solener.2015.06.028

Michael, J. J., & Iniyan, S. (2015b). Performance analysis of a copper sheet laminated photovoltaic thermal collector using copper oxide – water nanofluid. *Solar Energy*, *119*, 439–451. https://doi.org/10.1016/j.solener.2015.06.028

Moradi, K., Ali Ebadian, M., & Lin, C. X. (2013). A review of PV/T technologies: Effects of control parameters. *International Journal of Heat and Mass Transfer*, *64*, 483–500. https://doi.org/10.1016/j.ijheatmasstransfer.2013.04.044

Ngo, C. X., Do, N. Y., & Vuong, Q. (2022). Modeling and Experimental Studies on Water Spray Cooler for Commercial Photovoltaic Modules. *International Journal of Renewable Energy Development*, *11*(4), 926–935. https://doi.org/10.14710/ijred.2022.46209

Nijmeh, S., Yaseen, A. B., Ashhab, M. S., & Juaidy, M. (2022). Numerical Investigation of a Solar PV/T Air Collector Under the Climatic Conditions of Zarqa, Jordan. *International Journal of Renewable Energy Development*, *11*(4), 963–972. https://doi.org/10.14710/ijred.2022.45306

Peng, C., Huang, Y., & Wu, Z. (2011). Building-integrated photovoltaics (BIPV) in architectural design in China. *Energy and Buildings*, *43*(12), 3592–3598. https://doi.org/10.1016/j.enbuild.2011.09.032

PicoTech. (2021). *PT-104 Data Logger*. Online. https://www.picotech.com/download/datasheets/usb-pt-104-prt-data-logger-data-sheet.pdf

Qeays, I. A., Yahya, S. M., Asjad, M., & Khan, Z. A. (2020). Multi-performance optimization of nanofluid cooled hybrid photovoltaic thermal system using fuzzy integrated methodology. *Journal of Cleaner Production*, *256*, 120451. https://doi.org/10.1016/j.jclepro.2020.120451

Ragab, S., Saidani-scott, H., & Ezzat, O. (2019). Performance analysis for hybrid PV / T system using low concentration MWCNT (water-based) nano fl uid. *Solar Energy*, *181*(October 2018), 108–115. https://doi.org/10.1016/j.solener.2019.01.088

Raggie. (2021). *RAGGIE-mono-solar-panel*. Online. https://www.raggie.net/Content/upload/pdf/202024380/RAGGIE-mono-solar-panel.pdf?rnd=238

Rahmanian, S., & Hamzavi, A. (2020). Effects of pump power on performance analysis of photovoltaic thermal system using CNT nanofluid. *Solar Energy*, *201*(August 2019), 787–797. https://doi.org/10.1016/j.solener.2020.03.061

Said, Z., Arora, S., & Bellos, E. (2018). A review on performance and environmental effects of conventional and nano fluid-based thermal photovoltaics. *Renewable and Sustainable Energy Reviews*, *94*(October 2017), 302–316. https://doi.org/10.1016/j.rser.2018.06.010

Salari, A., Taheri, A., Farzanehnia, A., Passandideh-fard, M., & Sardarabadi, M. (2021). An updated review of the performance of nanofluid-based photovoltaic thermal systems from energy, exergy, economic, and environmental (4E) approaches. *Journal of Cleaner Production*, *282*, 124318. https://doi.org/10.1016/j.jclepro.2020.124318

Sardarabadi, M., Passandideh-fard, M., & Zeinali, S. (2014). Experimental investigation of the effects of silica / water nano fl uid on PV / T (photovoltaic thermal units). *Energy*, *66*, 264–272. https://doi.org/10.1016/j.energy.2014.01.102

Skoplaki, E., & Palyvos, J. A. (2009). On the temperature dependence of photovoltaic module electrical performance: A review of efficiency/power correlations. *Solar Energy*, *83*(5), 614–624. https://doi.org/10.1016/j.solener.2008.10.008

Tan, D., & Seng, A. K. (2011). Handbook for solar photovoltaic (pv) systems. *Singapore: Energy Market Authority*. https://policy.asiapacificenergy.org/node/172

Tiwari, A., & Sodha, M. S. (2006). Performance evaluation of solar PV/T system: An experimental validation. *Solar Energy*, *80*(7), 751–759. https://doi.org/10.1016/j.solener.2005.07.006

Tripanagnostopoulos, Y., Nousia, T., Souliotis, M., & Yianoulis, P. (2002). Hybrid photovoltaic/thermal solar systems. *Solar Energy*, *72*(3), 217–234. https://doi.org/10.1016/S0038-092X(01)00096-2

Varmira, K., Baseri, M. M., Khanmohammadi, S., Hamelian, M., & Shahsavar, A. (2021). Experimental study of the effect of sheet-and-sinusoidal tube collector on the energetic and exergetic performance of a photovoltaic-thermal unit filled with biologically synthesized water/glycerol-silver nanofluid. *Applied Thermal Engineering*, *186*(December 2020), 116518. https://doi.org/10.1016/j.applthermaleng.2020.116518

Younis, A., & Alhorr, Y. (2021). Modeling of dust soiling effects on solar photovoltaic performance: A review. *Solar Energy*, *220*(March), 1074–1088. https://doi.org/10.1016/j.solener.2021.04.011

Zhang, X., Zhao, X., Smith, S., Xu, J., & Yu, X. (2012). Review of R & D progress and practical application of the solar photovoltaic / thermal (PV / T) technologies. *Renewable and Sustainable Energy Reviews*, *16*(1), 599–617. https://doi.org/10.1016/j.rser.2011.08.026

Zhao, J., Song, Y., Lam, W., Liu, W., Liu, Y., Zhang, Y., & Wang, D. (2011). Solar radiation transfer and performance analysis of an optimum photovoltaic / thermal system. *Energy Conversion and Management*, *52*(2), 1343–1353. https://doi.org/10.1016/j.enconman.2010.09.032

© 2023. The Author(s). This article is an open access article distributed under the terms and conditions of the Creative Commons Attribution-ShareAlike 4.0 (CC BY-SA) International License (http://creativecommons.org/licenses/by-sa/4.0/)